Structure of nanocrystalline materials using atomic pair distribution function analysis: Study of $LiMoS_2$

V. Petkov,[1] S. J. L. Billinge,[1] P. Larson,[1] S. D. Mahanti,[1] T. Vogt,[2] K. K. Rangan,[3] and M. G. Kanatzidis[3]
[1]*Department of Physics and Astronomy and Center for Fundamental Materials Research, Michigan State University, East Lansing, Michigan 48824*
[2]*Physics Department, Brookhaven National Laboratory, Upton, New York 11973*
[3]*Department of Chemistry and Center for Fundamental Materials Research, Michigan State University, East Lansing, Michigan 48824*
(Received 6 December 2001; published 14 February 2002)

The structure of $LiMoS_2$ has been experimentally determined. The approach of atomic pair distribution function analysis was used because of the lack of well-defined Bragg peaks due to the short structural coherence (~50 Å) in this intercalation compound. The reduction of Mo by Li results in Mo-Mo bonding with the formation of chains of distorted Mo-S_6 octahedra. Using refined structural parameters the electronic band structure for this material has been calculated and is in good agreement with observed material properties.

DOI: 10.1103/PhysRevB.65.092105 PACS number(s): 61.43.−j

Knowledge of the atomic-scale structure is an important prerequisite to understand and predict the physical properties of materials. In the case of crystals it is obtained solely from the positions and intensities of the Bragg peaks in the diffraction data and is given in terms of a small number of atoms placed in a unit cell subjected to symmetry constraints.[1] However, many materials of technological importance are not perfect crystals and have diffraction patterns with a pronounced diffuse component and few Bragg peaks. In this case traditional crystallography fails. For completely disordered materials, such as glasses and liquids, a statistical description of the structure is often adopted. However, many materials lack perfect long-range order and yet have well-defined structures on nanometer-length scales (nanocrystals). In this case a description of the atomic structure, in terms of a unit cell and symmetry, can be achieved by employing a nontraditional experimental approach going beyond the Bragg scattering in the diffraction data. An important example is $LiMoS_2$. MoS_2 is the key catalyst for the removal of sulfur from crude oil (hydrodesulfurization).[2] Pristine MoS_2 is perfectly crystalline and consists of layers of Mo-S_6 trigonal prisms held together by van der Waals forces. $LiMoS_2$ has Li intercalated between the MoS_2 layers. It is important as a precursor of stable MoS_2 colloids used to prepare a variety of lamellar nanocomposites.[3] Despite being extensively studied for the last two decades[3–6] the structure of $LiMoS_2$ has not been determined. The reason is that, on Li intercalation, pristine MoS_2 is dramatically modified resulting in a product that is too poorly diffracting to allow a traditional structural determination. This leaves unanswered the important question of what exactly happens when MoS_2 gets reduced with Li. Theoretical predictions[5] and x-ray absorption fine-structure (XAFS) studies[6] suggest the presence of considerable Mo-Mo bonding but to our best knowledge, no unequivocal experimental evidence has been advanced so far. Here we use the atomic pair distribution function (PDF) technique to solve the structure of $LiMoS_2$. This approach has been used widely to study the structure of amorphous materials[7] and to find local structural deviations from a well-defined average structure.[8] Here we demonstrate that it also can be used to solve previously unknown structures of poorly diffracting, disordered, and nanocrystalline materials. We report a complete structural determination of $LiMoS_2$.

We find that the structural coherence is limited to ~50 Å in $LiMoS_2$ and, in this sense, the material is nanocrystalline. Nevertheless, it has a well-defined local structure with Mo atoms residing in distorted octahedra of sulfur. Short and long Mo-Mo distances appear indicative of metal-metal bonding that is theoretically predicted and easily understood in terms of simple electron counting arguments. Using the experimentally derived atomic coordinates we have calculated the electronic band structure that suggests $LiMoS_2$ is, in fact, a narrow band-gap semiconductor in good agreement with observation.

The atomic PDF is a function that gives the number of atoms in a spherical shell of unit thickness at a distance r from a reference atom. It peaks at characteristic distances separating pairs of atoms and thus reflects the structure of materials. The PDF $G(r)=4\pi r[\rho(r)-\rho_0]$ is the sine Fourier transform of the so-called total scattering structure function $S(Q)$,

$$G(r)=(2/\pi)\int_{Q=0}^{Q_{\max}} Q[S(Q)-1]\sin(Qr)dQ, \qquad (1)$$

where ρ_0 is the average atomic number density, $\rho(r)$ the atomic pair density, Q the magnitude of the scattering vector, and $S(Q)$ is the corrected and properly normalized powder-diffraction pattern of the material.[7] As can be seen from Eq. (1), $G(r)$ is simply another representation of the diffraction data. However, exploring the experimental data in real space is advantageous, especially in the case of materials with reduced long-range order. First, as Eq. (1) implies, the *total* scattering, including Bragg as well as diffuse scattering, contributes to the PDF. In this way all diffracted intensities are considered on the same footing, which is critical in the case of nanocrystalline materials, such as $LiMoS_2$, where the distinction between Bragg and diffuse scattering is not clear. Second, by accessing high values of Q, experimental PDF's of high real-space resolution can be obtained that reveal fine structural features.[9] Third, the PDF is obtained with no as-

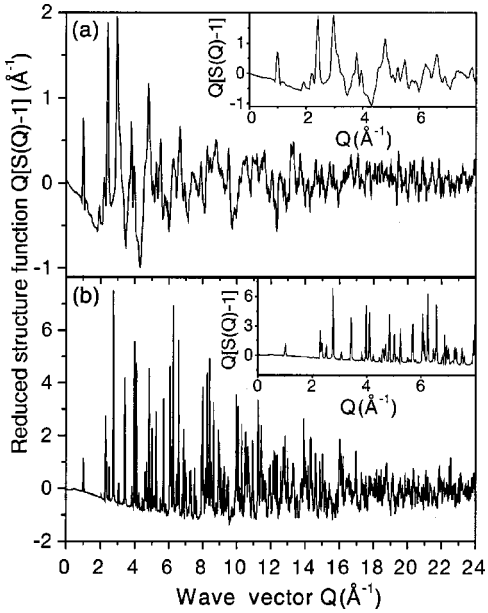

FIG. 1. Experimental structure functions of (a) $LiMoS_2$ and (b) MoS_2. Note the different scale between (a) and (b). The data are shown in an expanded scale in the insets.

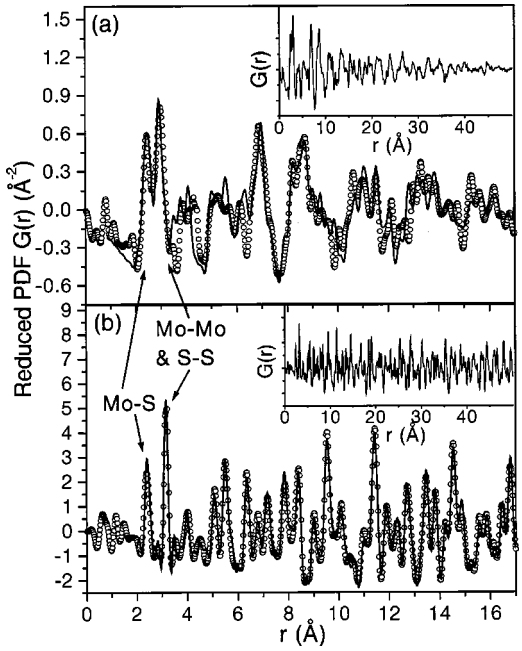

FIG. 2. Experimental (dots) and fitted (solid line) PDF's for $LiMoS_2$ (a) and MoS_2 (b). Note the different scale between (a) and (b). The first two peaks in the PDF's are labeled with the corresponding atomic pairs. The experimental data are shown in an expanded scale in the insets.

sumption of periodicity. Thus materials of various degrees of long-range order, ranging from perfect crystals to glasses and liquids, can be studied using the same approach. Finally, the PDF is a sensitive structure-dependent quantity giving directly the relative positions of atoms in materials. This, as demonstrated in the present paper, enables the convenient testing and refinement of structural models.

Two samples were investigated. One was pristine MoS_2 purchased from CERAC. The second was $LiMoS_2$ obtained by reacting pristine MoS_2 with excess $LiBH_4$.[2] The two powder samples were carefully packed between Kapton foils to avoid texture formation and subjected to diffraction experiments using x rays of energy 29.09 keV (λ=0.4257 Å). The measurements were carried out in symmetric transmission geometry at the beamline X7A of the National Synchrotron Light Source (NSLS), Brookhaven National Laboratory. Scattered radiation was collected with an intrinsic germanium detector connected to a multichannel analyzer. The raw diffraction data were corrected for flux, background, Compton scattering, and sample absorption. They were then normalized to obtain the structure function $S(Q)$.[7] All data processing was done using the program RAD.[10] Experimental structure functions are shown in Fig. 1 on an absolute scale and their Fourier transforms, the PDF's $G(r)$, in Fig. 2.

Sharp Bragg peaks are present in the $S(Q)$ of MoS_2 up to the maximal Q value of 24 Å^{-1} [Fig. 1(b)]. The corresponding $G(r)$ also features sharp peaks reflecting the presence of well-defined coordination spheres in this "perfectly" crystalline material [Fig. 2(b)]. The well-known six-atom hexagonal unit cell of MoS_2 (Ref. 11) was fit to the experimental PDF and the structure parameters refined so as to obtain the best agreement between the calculated and experimental data. The fit was done with the program PDFFIT (Ref. 12) and was constrained to have the symmetry of the $P6_3/mmc$ space group. In comparing with experiment, the model PDF was convoluted with a *Sinc* function to account for the finite Q_{max} of the measurement. The best fit achieved is shown in Fig. 2(b) and the corresponding value of the goodness-of-fit indicator R_{wp} is 21%.[13] The unit cell of MoS_2 was also fit to the powder-diffraction data using the Rietveld technique. All refinement results are summarized in Table I and the agreement with the published crystallographic results[11] is very good.

We turn now to the $LiMoS_2$ data. In this material the Bragg peaks are significantly broadened [see the inset in Fig. 1(a)] and already at ~8 Å^{-1} merge into a slowly oscillating diffuse component. A diffraction pattern so poor in sharp Bragg peaks lacks the number of "statistically independent reflections"[14] needed to apply the traditional techniques for structure determination. The corresponding PDF is, however, rich in distinct, structure-related features and, as we will see, lends itself to structure determination. In the inset in Fig. 2(a) it is evident that the features in the PDF disappear at 50 Å. In this sense, $LiMoS_2$ is nanocrystalline. However, its local structure is still relatively well defined with clearly iden

TABLE I. Structural parameters for MoS_2. Space group is $P6_3/mmc$. Mo is at ($\frac{1}{3}$, $\frac{2}{3}$, $\frac{1}{4}$) and S at ($\frac{1}{3}$, $\frac{2}{3}$, z).

	PDF	Rietveld	Single crystal[a]
a (Å)	3.169(1)	3.168(1)	3.1604(2)
c (Å)	12.324(1)	12.322(1)	12.295(2)
z	0.623(1)	0.625(1)	0.629(1)

[a]Reference 11.

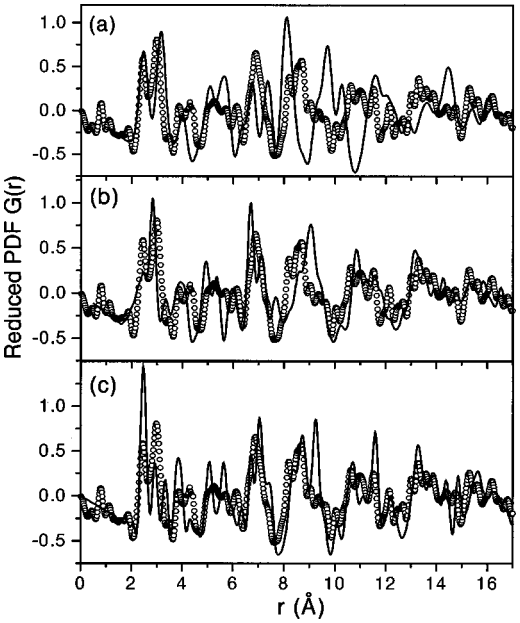

FIG. 3. Comparison between the experimental PDF for $LiMoS_2$ (symbols) and model PDF's (full line) for (a) hypothetical hexagonal $LiMoS_2$, (b) hypothetical $1T$-$LiMoS_2$, and (c) triclinic $LiMoS_2$ as predicted in Ref. 5.

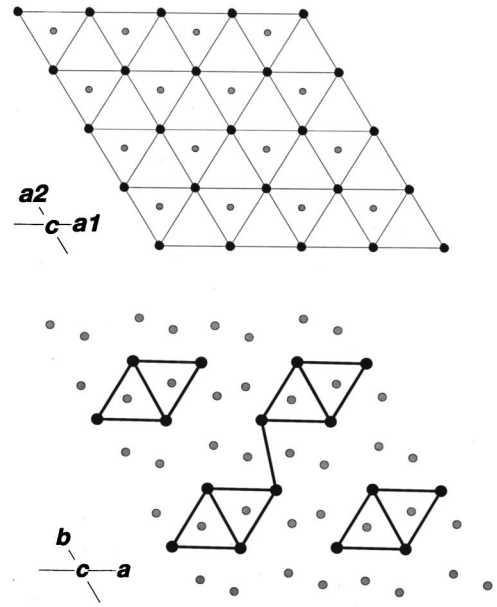

FIG. 4. Projection down the c axis of the crystal structures of hexagonal MoS_2 (up) and triclinic $LiMoS_2$ (down). The large black circles are Mo atoms and the small gray circles are the S atoms. Li atoms are not shown for the sake of clarity.

tifiable Mo-S and Mo-Mo coordination spheres as seen in Fig. 2(a). The structural features persist to much higher r values in the pristine MoS_2 [see the inset in Fig. 2(b)], which is a macroscopic crystal.

To determine the parameters of the atomic structure of $LiMoS_2$ we explored several structure models as follows: First, a model based on the hexagonal MoS_2 structure (space group $P6_3/mmc$) was attempted. It was constructed by inserting two Li atoms into the six-atom unit cell of MoS_2 so that they resided between the Mo-S_2 layers. This model, however, could not reproduce the experimental data as can be seen in Fig. 3(a). A previously proposed[4] structure for $LiMoS_2$ is based on trigonal $1T$-MoS_2 (space group $P3$), which can be considered as built of layers of distorted Mo-S_6 octahedra. This structure model was also tested with the starting structure parameters, lattice constants, and atomic coordinates of Mo and S, being those reported in Ref. 6. Again Li atoms were added to occupy appropriate sites between the Mo-S_2 layers. The model performed somewhat better but still could not reproduce the details in the experimental PDF as can be seen in Fig. 3(b). Therefore $LiMoS_2$ and $1T$-MoS_2 are not exactly of the same structure type, contrary to what has been suggested before.[4] Next we attempted a model based on the "exfoliated-restacked" MS_2 structure (M=W,Mo) (Ref. 15), which features zigzag metal-metal chains. This was an excellent starting point and as the refinement proceeded the Mo atoms shifted slightly but significantly to new positions that define the chains of Mo atoms shown in Fig. 4. This model fits all the important details in the experimental PDF as can be seen in Fig. 2(a). The refined structure parameters are summarized in Ref. 16. The agreement with the data is less satisfactory than with the MoS_2; however, this model is significantly better than either of the previously proposed models. Given the high degree of disorder inherent in $LiMoS_2$ this level of agreement is quite good and acceptable.

In pristine MoS_2 Mo atoms from a single MoS_2 layer arrange in a regular hexagonal lattice (see Fig. 4) and are all separated by the same distance of 3.16 Å. In contrast, the Mo atoms in $LiMoS_2$ occupy two distinct positions in the triclinic unit cell[16] giving rise to short (2.9–3.10 Å) and long (3.44–4.07 Å) Mo-Mo distances. As a result, a chain-of-diamonds motif of bonded Mo atoms emerges (Fig. 4). This is in qualitative agreement with the structure proposed in an earlier XAFS study[6] and predicted theoretically,[5] though the details are significantly different. The "diamond-chain" model is easy to understand using simple electron counting arguments.

In MoS_2 molybdenum is in the 4+ state and has two d electrons. It is most stable in a prismatic crystal field resulting in a 1-2-1-1 arrangement of atomic d energy levels. The two electrons both occupy the lowest-energy d_{z^2} level, which is therefore nonbonding. When Mo gets reduced by the addition of Li it has three d electrons. The prismatic coordination is destabilized with respect to octahedral coordination that results in triply degenerate t_{2g} and doubly degenerate e_g levels. One electron goes into each of the three t_{2g} levels, which point towards neighboring Mo ions. Each Mo can then form bonding interactions with three of its neighboring Mo ions resulting in three shorter and three longer Mo-Mo distances and the diamondlike pattern of distortions shown in Fig. 4.

Using the atomic coordinates determined in this study[16] we calculated the electronic band structure using the full-potential plane-wave method within density-functional theory.[17] As can be seen in Fig. 5 a gap of about 0.2 eV is present in the electronic density of states at the Fermi level.

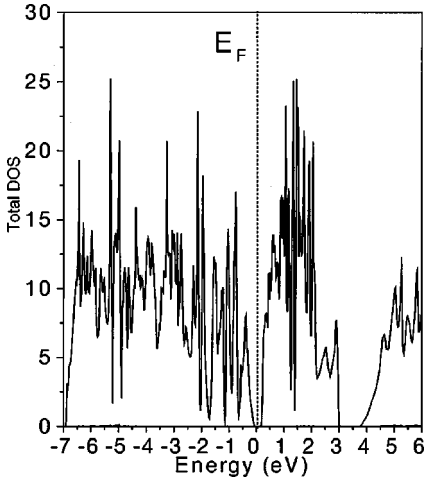

FIG. 5. Total density of states for $LiMoS_2$.

The material should exhibit semiconducting properties as observed.[4] By comparison, in pristine MoS_2 the band gap is 1.4 eV.

A recent first-principles calculation predicted a triclinic (space group $P\bar{1}$) unit cell for $LiMoS_2$ with Mo atoms arranged in a ''diamond-chain'' scheme resulting in a 1-eV gap.[5] A comparison between the PDF for the theoretically predicted structure of $LiMoS_2$ and the experimental PDF is shown in Fig. 3(c). The agreement between the two PDF's is satisfactory but the predicted structure does not do as well as our structural solution [see Fig. 2(a)]. Nevertheless, both the present and the previous theoretical studies seem in agreement on the essential structural features of $LiMoS_2$.

In conclusion we have shown that the atomic PDF approach can be confidently employed to solve the structure of nanocrystalline materials. Key to the success of this approach is that both Bragg and the diffuse component of diffraction data are collected over a wide range of wave vectors before being converted into the corresponding PDF. Then, like all powder-diffraction techniques, the three-dimensional structure is inferred through modeling. The PDF approach provides a major advantage since it yields the atomic structure in terms of a unit cell and symmetry even when materials are not perfect crystals and diffraction data show only a few Bragg peaks.

This work was supported by National Science Foundation Grant Nos. CHE 99-03706 and DMR-9817287, and DARPA Grant No. DAA 695-97-0184. The NSLS is supported by the US Department of Energy through Grant No. DE-AC02-98-CH10886.

[1] M. M. Woolfson, *An Introduction to X-Ray Crystallography* (Cambridge University, Cambridge, England, 1997).

[2] M. G. Kanatzidis, R. Bissesssur, and D. C. DeGroot, Chem. Mater. **5**, 595 (1993); H.-L. Tsai, J. Heising, J. L. Schindler, C. R. Kannewurf, and M. G. Kanatzidis, *ibid.* **9**, 879 (1997).

[3] W. M. R. Divigalpitiya, R. F. Frindt, and S. R. Morrison, Science **246**, 369 (1989).

[4] M. A. Py and R. Haering, Can. J. Phys. **61**, 76 (1983); P. Mulhern, *ibid.* **67**, 1049 (1989).

[5] X. Rocquefelte, F. Boucher, P. Gressier, G. Ouvrard, P. Blaha, and K. Schwartz, Phys. Rev. B **62**, 2397 (2000).

[6] K. E. Dungey, M. D. Curtis, and D. E. Penner-Hahn, Chem. Mater. **10**, 2152 (1998); S. Lemaux, A. Golub, P. Gressier, and G. Ouvrard, J. Solid State Chem. **147**, 336 (1999).

[7] H. P. Klug and L. E. Alexander, *X-Ray Diffraction Procedures for Polycrystalline Materials* (Wiley, New York, 1974).

[8] T. Egami, Mater. Trans., JIM **31**, 163 (1990); S. J. L. Billinge, R. G. DiFrancesco, G. H. Kwei, J. J. Neumeier, and J. D. Thompson, Phys. Rev. Lett. **77**, 715 (1996); S. Teslic and T. Egami, Acta Crystallogr., Sect. B: Struct. Sci. **54**, 750 (1998); M. Tucker, M. Dove, and D. A. Keen, J. Phys.: Condens. Matter **12**, L723 (2000).

[9] V. Petkov, I-K. Jeong, J. S. Chung, M. F. Thorpe, S. Kycia, and S. J. L. Billinge, Phys. Rev. Lett. **83**, 4089 (1999); V. Petkov, S. J. L. Billinge, S. D. Shastri, and B. Himmel, *ibid.* **85**, 3436 (2000).

[10] V. Petkov, J. Appl. Crystallogr. **22**, 387 (1989).

[11] R. Wyckoff, *Crystal Structures* (Wiley, New York, 1964).

[12] Th. Proffen and S. J. L. Billinge, J. Appl. Crystallogr. **32**, 572 (1999).

[13] Note the R_{wp} for the PDF fit is defined in Ref. 12. While the definition is similar to that used in Rietveld refinements the functions being fit are significantly different and the R_{wp}'s should not be to compared directly between PDF and Rietveld refinements. However, they are useful as a measure for goodness of fit when comparing different models fit to the same PDF data. PDF R_{wp}'s greater than 10% from well-crystallized samples are not uncommon.

[14] D. S. Silva, J. Appl. Crystallogr. **33**, 1295 (2000).

[15] V. Petkov, S. J. L. Billinge, J. Heising, and M. G. Kanatzidis, J. Am. Chem. Soc. **122**, 11 571 (2000).

[16] Structure parameters of $LiMoS_2$: $a=6.963(1)$, $b=6.386(1)$, $c=6.250(1)$ Å, $\alpha=88.60°$, $\beta=89.07°$, and $\gamma=120.06°$; space group $P\bar{1}$: Mo1 (0.9187, 0.7251, 0.4977); Mo2 (0.506, 0.7342, 0.5138); S1 (0.6638, 0.5628, 0.7863); S2 (0.1349, 0.0158, 0.771); S3 (0.6979, 0.0736, 0.7441); S4 (0.1033, 0.5369, 0.7569); Li1 (0.03, 0.7481, 0.013); Li2 (0.537, 0.7356, 0.009); $R_{wp}=29\%$ (Ref. 13).

[17] P. Hohenberg and W. Kohn, Phys. Rev. B **136**, 864 (1964); J. P. Perdew, K. Burke, and M. Ernzerhof, Phys. Rev. Lett. **77**, 3865 (1996); P. Blaha, K. Schwarz, and J. Luitz, Computer code WIEN97, Technical University of Vienna, 1997.